Jour. of the KGS, Vol. 20, No. 2. March 2004, pp. 47~58

Loss Estimation of Steel Pipeline Damage in Los Angeles Using GIS

GIS를 이용한 로스엔젤레스에 매설된 강관 손상 평가

Jeon, Sang-Soo[1] 전 상 수

요 지

강관은 Northridge 지진이 발생했을 당시 산사태가 일어나는 언덕이나 산악지역에 매설되어 있었다. 본 논문은 지리정보체계(GIS) 시스템에서 위치에 따라 강관을 서로 다른 유형별로 분류하고 정의하였다. 이 논문은 지반속도와 강관의 손상관계를 분석하고 Northridge 지진 시 발생한 산사태의 영향을 받았던 지역을 조사하였다. 하나의 주목할 만한 사실은 Northridge 지진 후 강관의 손상률이 다른 종류의 매설관, 특히 캐스트아이런(CI)보다 더 높았다는 것이다. Northridge 지진으로 인한 상대적으로 높은 강관의 손상률은 가장 큰 내부압력을 요하는 곳에서의 설치관례와 부식으로 인한 영향으로 해석될 수 있다.

Abstract

Steel Pipelines were located in hillside and mountain areas where landslides occurred during the Northridge earthquake. This paper describes the investigations that were performed to identify and locate the different types of steel pipeline construction in the system using GIS (Geographical Information System). The paper explores the damage correlations of steel pipelines with PGV (peak ground velocity) and investigates the areas subjected to the landslide effects during the Northridge earthquake. One noticeable finding is that the repair rates for steel distribution pipelines after the Northridge earthquake are higher than those of CI (cast iron) pipelines. The relatively high susceptibility of steel piping to damage during the Northridge earthquake may be explained in part by utility practices, such as using steel pipe for the highest internal pressures, and increased susceptibility to corrosion also appears to play a role in steel pipeline performance.

Keywords : Earthquake, GIS, Landslide, Pipelines, Slope stability

1. Introduction

This paper focuses on the spatial damage characteristics of steel pipelines in the LADWP (Los Angeles Department of Water and Power) water distribution system after the 1994 Northridge earthquake. Steel pipelines were distributed over the mountain and hillside areas and if they are composed of steel, irrespective of fabrication, characteristics, and type of joints, they were listed generically as "steel" pipelines. Damage of steel pipeline invites a question about its relationship with earthquake parameter, peak ground velocity (PGV). Steel pipelines were buried in the areas in which landslides occurred during the Northridge earthquake. The landslide activities were observed in Sherman Oaks and Mount Olympus areas in the City of Los Angeles (Tan, 1995; Dekermenjian, 2000).

This paper describes the investigations that were performed to identify and locate the different types of steel pipeline construction in the system using GIS. The

1 Member, Chief Researcher, Korea Highway & Transportation Technology, Korea Highway Corporation (ssj3@freeway.co.kr)

paper investigates the damage correlations of steel pipelines with PGV in the areas subjected to the landslide effects. The paper presents a description of slope analyses and the method of Newmark's block sliding that were developed to simulate landslide displacement (Jeon, 2002). The damage correlations of steel pipelines with the angle of slope and landslide displacement are presented and explained.

2. Steel Pipeline Characteristics

Fig. 1 shows the density of steel pipelines expressed as contour lines with a contour interval of 1.0 km of pipeline per km^2. The contour intervals were generated by overlaying a 2 km x 2 km mesh onto the steel pipeline distribution system (O'Rourke and Toprak, 1997; Toprak, 1998). The length of pipelines in each cell of the 2 km x 2 km mesh was divided by the cell area to provide a normalized length. Contours were drawn from the spatial distribution of normalized lengths, each of which was centered on each cell. The contour interval is 1.0 km per km^2. As shown in Fig. 1, steel pipelines are concentrated mostly in areas with significant slopes and elevated topography. They constitute the outermost parts of the water distribution system at several locations in the mountains. Because of their perceived strength and ductility steel pipelines are installed by LADWP in areas that are susceptible to ground deformation caused by slope instability and differential settlement at the margins of cut and fill construction.

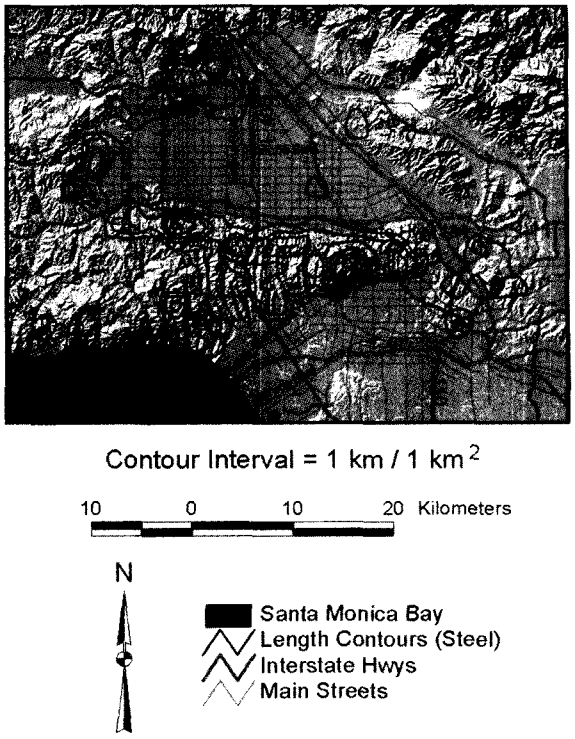

Fig. 1. Pipeline length contours for steel distribution pipelines (after O'Rourke and Toprak, 1997; Toprak, 1998)

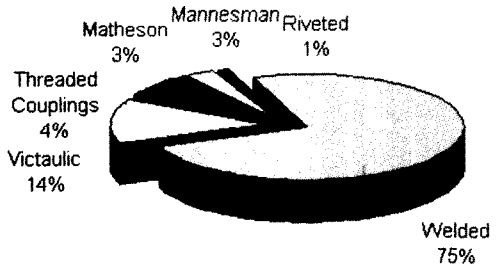

Total pipeline length: 1018 km
(a) Steel pipeline length

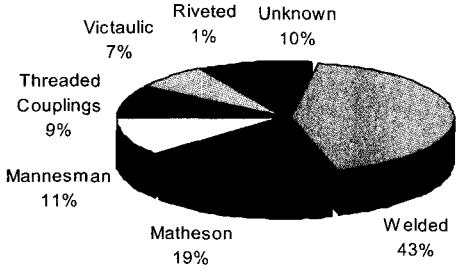

Total repairs: 205
(b) Steel pipeline repairs

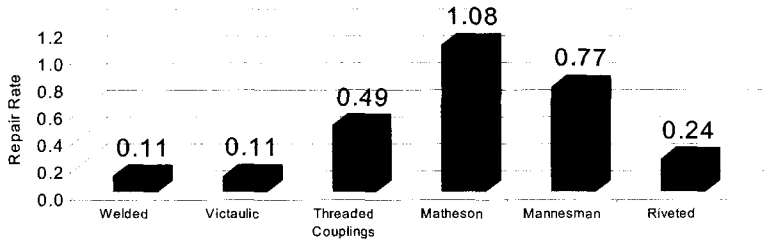

(c) Steel pipeline repair rate

Fig. 2. Steel pipeline repairs, length, and repair rate related to composition

The information initially available from LADWP did not distinguish different types of steel pipeline construction. All pipelines composed of steel, irrespective of fabrication, steel characteristics, and type of joints, were listed generically as "steel" pipelines. It was necessary, therefore, to perform additional investigations to identify and locate the different types of steel pipeline construction in the system.

Working with LADWP engineers, the roughly 1,000 km of pipelines, initially identified as "steel", were divided into six categories, including pipelines with welded slip joints, Victaulic couplings, threaded couplings, riveted steel, and Matheson and Mannesman steel. The lengths associated with each type of pipe were located on LADWP maps and then geocoded into the GIS of the pipeline system by means of map digitizing equipment.

Fig. 2(a) presents a pie chart showing the relative percentages of the LADWP steel distribution pipelines associated with different types of pipe. Figs. 2(b) and 2(c) show the distribution of steel pipe repairs and repair rate, respectively, according to pipe type. The highest concentrations of steel pipeline repairs are associated with Mannesman and Matheson steel, which are prone to corrosion, as well as certain types of elastometric joints (Victaulic couplings) that are vulnerable to creep and leakage. About 37% of all steel pipeline repairs occurred in Mannesman, Matheson, and Victaulic pipelines. These types of pipeline constitute only 7% of steel pipelines in the system.

Matheson and Mannesman steel pipelines were installed primarily in the 1920s and 1930s. Most were installed without cement linings and with minimal coating. In addition, their wall thickness is generally less than that of other steel pipes with similar diameter.

Matheson and Mannesman steel pipelines are vulnerable to corrosion, as are steel pipelines with threaded couplings. In the latter case, corrosion tends to concentrate at the threaded cross-sections. These types of pipelines did not perform well during previous U.S. and Japanese earthquakes (Katayama and Isoyama, 1980; Eguchi, 1982; O'Rourke, et al., 1985).

Victaulic couplings are bolted, segmental, clamp-type mechanical couplings that enclose a U-shaped rubber gasket (American Water Works Association, 1964). The gasket tends to deform and lose its initial water-tight characteristics under prolonged service. Riveted steel pipelines are older installations, which are prone to corrosion. Contact between the rivets and laminated steel of the pipe body promotes galvanic action between the two dissimilar metals.

A welded slip joint (WSJ) is fabricated by inserting the straight end of one pipe into the bell end of another and joining the two sections with a circumferential fillet weld. The bell end is created by the pipe manufacturer by inserting a mandrel in one end of a straight pipe section, and expanding the steel into a flared, or bell casing. The pie charts in Fig. 2 show that this type of steel pipeline (referred to as welded) was the predominant type operated at the time of the Northridge earthquake.

3. Steel Pipeline Damage Patterns

Figs. 3 and 4 show the locations of pipeline repairs for the various types of steel pipe plotted with respect to the topography and street system and the spatial distribution of PGV, respectively. Repairs in the relatively flat areas of the San Fernando Valley were predominantly in the weakest types of piping, normally the Matheson pipelines. Repairs in the areas of elevated topography were principally in pipelines with threaded and welded slip joints.

As described by O'Rourke and Jeon (1999), the evaluation of pipeline repair rate relative to PGV depends on the length of pipeline associated with a given type of pipe, diameter, and PGV. If the pipeline length is very small, then the statistics of repair can be biased by anomalously high or low values depending on the presence or absence of concentrated damage. To provide a sufficiently large sample size to minimize such biases, it was found that a pipeline length, or sample size, equal to or greater than 2% of the total pipeline length is needed per correlation with PGV. No pipeline repairs were observed in areas with PGV < 10 cm/sec.

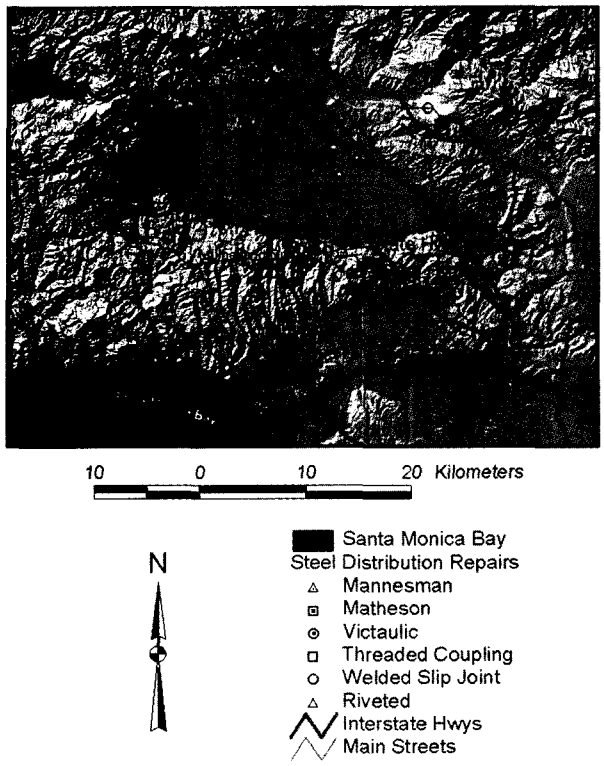

Fig. 3. Location of steel distribution pipeline repairs relative to topography and street system

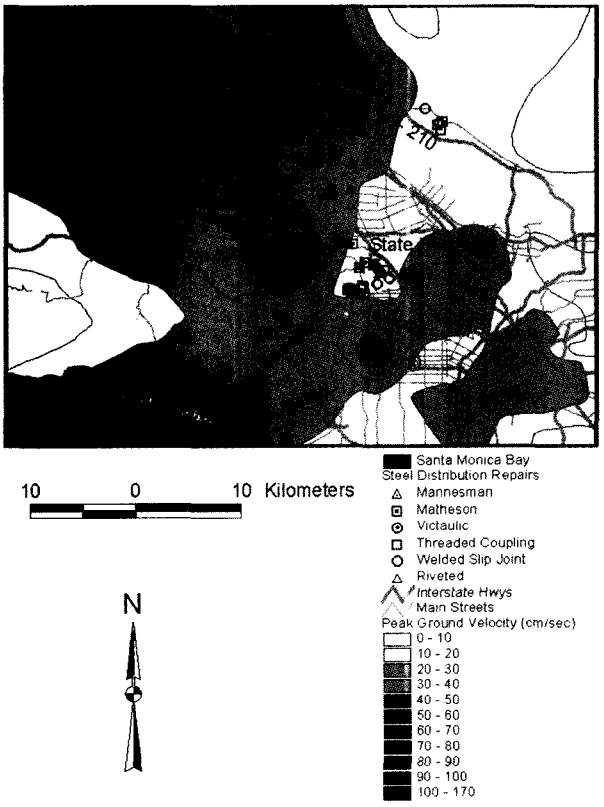

Fig. 4. Location of steel distribution pipeline repairs relative to PGV

The information illustrated in Fig. 2 shows that there were relatively small lengths of pipelines with Victaulic couplings, threaded couplings, riveted steel, and Mannesman and Matheson steel. These lengths were insufficient to provide a suitable sample size for each range of PGV shown in Fig. 4. The only type of steel pipeline for which there was sufficient length for statistically robust correlations was pipe with welded slip joints.

The overall repair rates in Fig. 2 are useful for showing the relative vulnerability of the different types of steel pipeline. Only the pipelines with welded slip joints, however, had sufficient length exposed to the effects of the Northridge earthquake to evaluate the relationship between repair rate and PGV.

4. Observations of Pipeline Damage and Slope Instability

Various investigators have reported on landslides and hillside instabilities at cut-and-fill zones triggered by the Northridge earthquake (Barrows, et al., 1995; Stewart, et al., 1996 and 1998; Tan, 1995; Jibson, et al., 1998). Barrows, et al. (1995) claimed that landslides were the most plentiful and widespread surface effects of the Northridge earthquake and that several formations in particular, were susceptible to deep-seated sliding, including the Modelo and Pico Formations. They mapped landslides and other ground failure phenomena throughout a total area corresponding to 2,880 mi^2 (7,500 km^2).

Significant ground deformations were described and discussed by Stewart, et al. (1996) in the San Fernando Valley communities of Granada Hills, Northridge, Sherman Oaks, and San Fernando. They described ground deformation triggered by landslides and liquefaction and related such deformation, where sufficient information was available, to residential housing and pipeline damage. Of particular interest are ground movements at cut-and-fill zones in hillsides, principally along the north flank of the Santa Monica mountains and north rime of the San Fernando Valley. The most common movement patterns in these zones consisted of cracks near cut/fill contacts, lateral extension, differential settlement of fills, and slumping at the face of fills.

Stewart, et al. (1998) reported that deformations at cut-and-fill zones were responsible for damage, primarily to residential structures, at over 2,000 sites for a combined loss exceeding $100 million. Damage to pipelines in cut-and-fill zones was also observed, but details about the extent and characteristics of such damage were generally not available to the investigators.

Landslide-related damage was especially severe in the Sherman Oaks area (Barrows, et al., 1995; Stewart, et al., 1996). Tan (1995) developed maps of the Sherman Oaks area showing zones of concentrated slope failure features such as rock falls, debris/soil falls, soil slides, and landslides. The maps also show zones of multiple ground fissures, including extensional cracks and step-like vertical offsets. Evidence of slippage along bedding planes on dip slopes was observed in many places. A regional pattern of joints contributed to increased damage along ridge tops, especially where the trend of the joints is parallel to linear ridges. Ground cracks, fissures, and heavy damage to pipelines were concentrated along head scarps and the upper portions of pre-existing landslides.

Jibson, et al. (1998) investigated ground deformation triggered by landslides in the Oat Mountain area, which includes parts of the northern San Fernando Valley and the Santa Susanna Mountains. The Oat Mountain area lies just a few kilometers north of the Northridge earthquake epicenter and contains a high concentration of landslides (Harp and Jibson, 1995 and 1996). Topography ranges from flat areas in the San Fernando Valley to nearly vertical slopes in the Santa Susana Mountains. Predominant geologic units in areas of the Oat Mountain include uncemented to weakly cemented, late Tertiary clastic sediments and well-cemented Cretaceous sandstone. They developed a method for predicting landslides caused by the Northridge earthquake and compared the predictions with the results with their observations. Additional information about the analytical procedures employed by Jibson, et al. (1998) in relating permanent ground deformation (PGD) to slopes is described in detail and related to pipeline repair rate.

PGD was observed in the Mount Olympus and adjacent areas after the earthquake (Dekermenjian, 2000). LADWP records between 1988 and 1994 show that pipeline repairs were affected by PGD in these areas, well before the Northridge earthquake.

5. Landslide Assessmeant

Jibson, et al. (1998) proposed a relationship among landslide displacement, Arias Intensity (AI), and critical acceleration (a_c). They used a large group of strong motion records (280 recording stations in 13 earthquakes) to develop a regression equation. They analyzed both horizontal components of acceleration from 275 recordings and a single component of an additional 5, which yielded 555 single component records. For each record, they determined the AI, a single numerical measure of the seismic intensity of the record calculated by integrating the squared acceleration values. Then Newmark analyses for several values of critical acceleration were conducted, ranging from 0.02g to 0.40g. The resulting Newmark displacements were then regressed on two predictor variables, critical acceleration and AI.

In this work the landslide displacement relationship of Jibson, et al. (1998) was used as an index for the combined effects of the angle of slope and seismic intensity. Using GIS, the angle of slope at various locations can be determined from DEM files using the estimation model of slope. The Arias Intensities (AI) at various locations in the LA region were estimated by O'Rourke, et al. (1998) and Toprak (1998), and the GIS files of AI developed by them were used in this work. Hence, explicit information about slope and AI was already available.

AI has been proposed as a measure to assess the liquefaction potential of soil deposits during earthquakes (Kayen, et al., 1994 and 1997). Introduced as a quantitative measure of earthquake intensity, AI is the total energy per unit weight dissipated by a set of one degree of freedom oscillators with viscous damping during the overall duration of earthquake motion (Arias, 1970). The total intensity related to motion on a horizontal plane can be obtained by summing the intensity values calculated from the two horizontal accelerograms (a_x and a_y, at right

angles to each other) as follows

$$AI_h = AI_{xx} + AI_{yy} = \frac{\pi}{2g}\int_0^{t_0} a_x^{\,2}(t)dt + \frac{\pi}{2g}\int_0^{t_0} a_y^{\,2}(t)dt \quad (1)$$

in which AI_{xx} is Arias Intensity along the x-directions, AI_{yy} is Arias Intensity along the y-directions, $a_x(t)$ is ground acceleration along the x-directions, $a_y(t)$ is ground acceleration along the y-directions, t_o is total duration of earthquake, and g is acceleration due to gravity. The dimension of AI is length/time.

A method for estimating the permanent ground displacement triggered by earthquake motion for a given slope was developed by Newmark (1965). Wilson and Keefer (1983) showed that using Newmark's method to model the dynamic behavior of landslides on natural slopes yields reasonable and useful results. Wieczorek, et al. (1985) subsequently produced a map showing seismic landslide susceptibility in San Mateo County, California, using classification criteria based on Newmark's method. Wilson and Keefer (1985) also used Newmark's method as a basis for a broad regional assessment of seismic slope stability in the Los Angeles area.

Fig. 5(a) shows Newmark's method modeling a landslide as a rigid block that slides on an inclined plane. The block has a known critical acceleration, a_c, which is simply the threshold base acceleration required to overcome shear resistance and initiate sliding. The analysis calculates the cumulative permanent displacement of the block relative to its base as it is subjected to the effects of an earthquake acceleration-time history.

In the analysis, an acceleration-time history is selected, and the critical acceleration (a_c) of the slope to be modeled is superimposed as shown in the Fig. 5(b). Acceleration below this level causes no permanent ground displacement of the block. Those portions of the record that exceed the critical acceleration (a_c) are integrated once to obtain the velocity profile of the block as shown in the Fig. 5(c). A second integration is performed to obtain the cumulative displacement history of the block shown in the Fig. 5(d).

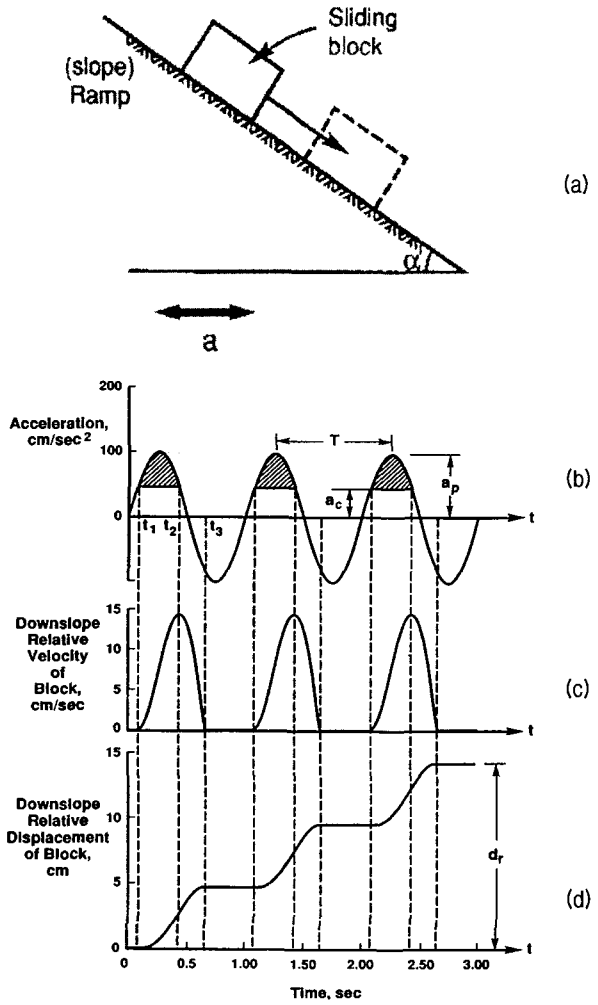

Fig. 5. Demonstration of the Newmark-analysis algorithm: (a) sliding-block model (b) earthquake acceleration-time story with critical acceleration (horizontal dashed line) of ac (c) velocity of landslide block vs. time (d) displacement of landslide block vs. time

The maximum resisting shear force on the plane, Rmax, can be expressed as

$$R_{max} = N \tan\phi' = W \cos\alpha \tan\phi' \quad (2)$$

in which N is the normal force on the plane, W is the weight of block, α is the angle of slope, and ϕ' is an angle of soil friction.

The driving force on the block is

$$S_{max} = W \sin\alpha \quad (3)$$

The value of static factor of safety (FS) against block sliding obtained by combining Eqs. 2 and 3 is

$$FS = \frac{\tan \phi'}{\tan \alpha} \quad (4)$$

The maximum shear resisting force required for static equilibrium is expressed as

$$T_{max} = W \sin \alpha + \frac{W}{g} a_c \quad (5)$$

Combining Eqs. 2, 4, and 5 results in

$$a_c = (FS - 1) g \sin \alpha \quad (6)$$

where a_c is the critical acceleration in terms of g, the acceleration of Earth's gravity; FS is the static factor of safety; and α is the angle of slope from the horizontal to the center of mass of the potential landslide.

The dynamic stability of a slope in Newmark's method is directly related to its static stability represented by the static factor of safety. A relatively simple limit equilibrium model of an infinite slope in material having both frictional and cohesive strength was used. The factor of safety (FS) can be written (Jibson, et al., 1998) as a function of effective cohesion, c', and the unit weight of water, γ_w, as

$$FS = \frac{\tan \phi'}{\tan \alpha} + f(c') - f(\gamma_w) \quad (7)$$

The FS is also function of c' and γ_w as shown in Fig. 6 and is written as

$$FS = \frac{\tan \phi'}{\tan \alpha} + \frac{c'}{\gamma t \sin \alpha} - \frac{m \gamma_w \tan \phi'}{\gamma \tan \alpha} \quad (8)$$

where ϕ' is the effective friction angle, γ is the soil unit weight, t is the slope normal thickness of the failure slab, and m is the proportion of the slab thickness that is saturated.

The equation is written so that the first term on the right side accounts for the frictional component of the strength, the second term accounts for the cohesive component, and the third term accounts for the reduction in frictional strength due to pore pressure. For simplicity, the effective cohesion was assumed to be zero; thus, the second term drops from the equation. Jibson, et al. (1998) found that most of landslide failures during the Northridge earthquake occurred under dry conditions. No pore-water pressure was included (m=0) for this analysis. Thus, the third term drops from the equation. The factor of safety, then, was calculated by inserting values for friction angle and the slope angle into Eq. 4.

Jibson, et al. (1998) developed a simplified Newmark method, which provides an empirical regression equation used to estimate landslide displacement as a function of seismic intensity and critical acceleration. The regression equation of landslide displacement is written as

$$Log(D_n) = 1.521\ Log(AI) - 1.993\ Log(a_c) - 1.546 \quad (9)$$

where D_n is landslide displacement in centimeters, AI is Arias Intensity in meters per second, and a_c is critical acceleration in g's. The regression equation was well constrained ($r^2 = 0.83$) with a very high level of statistical significance. The model standard deviation was 0.38. With Eq. 9, landslide displacement can be estimated as a function of critical acceleration and AI.

Fig. 6 shows a flow chart showing the sequential steps to derive landslide displacement for data layers consisting of 30 x 30 m raster grids of the entire 7.5-minute

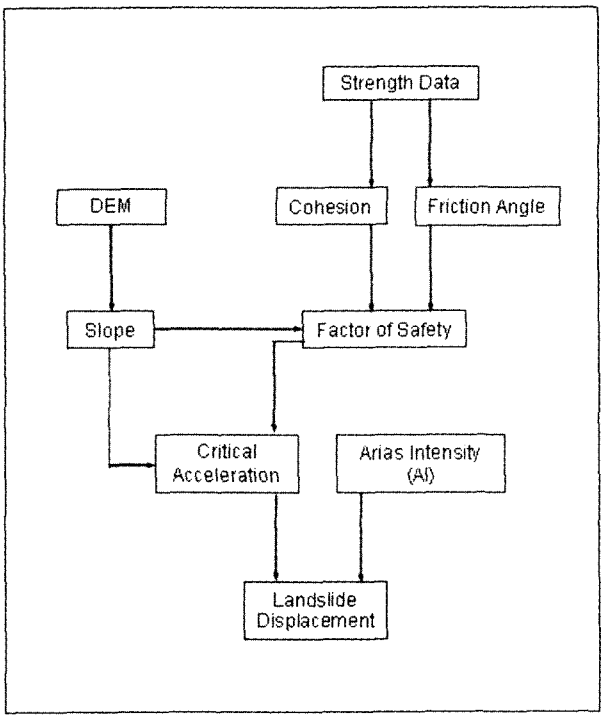

Fig. 6. Flow chart showing steps involved in producing a seismic landslide (after Jibson, et al., 1998)

quadrangle. The static factor of safety was calculated by assigning the representative shear strengths to each unit, which yields friction (ϕ') and cohesion (c') grids. A slope map from the DEMs was constructed. Shear strength and slope data were combined to estimate the static factor of safety in each grid cell. The critical acceleration was computed by combining the factor of safety grid with the slope grid to yield the critical-acceleration grid, which represents seismic landslide susceptibility. Landslide displacements were estimated using the empirical regression Eq. 9 to combine the critical accelerations and AI values from the Northridge earthquake.

6. Landslide Effects

To estimate a_c, various ϕ' were used to explore the statistical relationships among repair rate (RR), landslide displacement (D_n), and the sensitivity of these relationships to changes in ϕ'. Pipeline repair rate is defined as the number of repairs per km of pipeline for a specific pipe composition. Selecting a specific value of ϕ' introduces assumed strength variables into the assessment of D_n so that the resulting value of AI and slope, and only loosely tied to soil strength parameters. Testing the statistical robustness of regressions between RR and D_n for assumed ϕ', nevertheless, provides a measure of how much variability can be explained by knowledge of slope and AI and whether such an approach is potentially

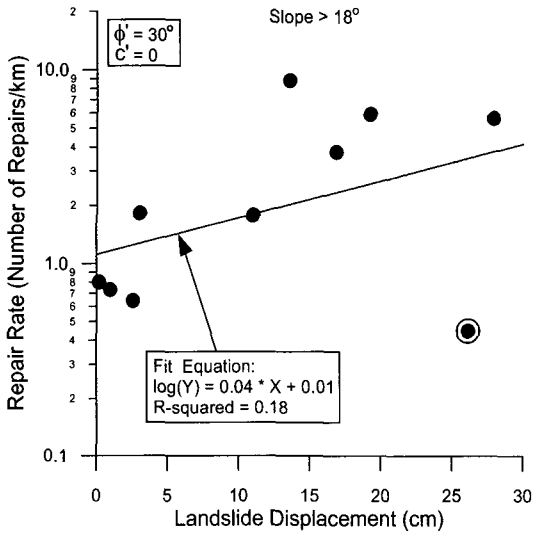

Fig. 7. WSJ steel pipeline repair rate correlation with landslide displacement

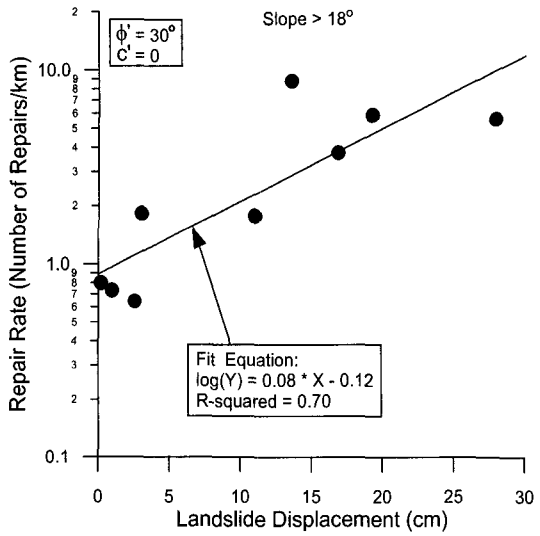

Fig. 9. WSJ steel pipeline repair rate correlation with landslide displacement without bias

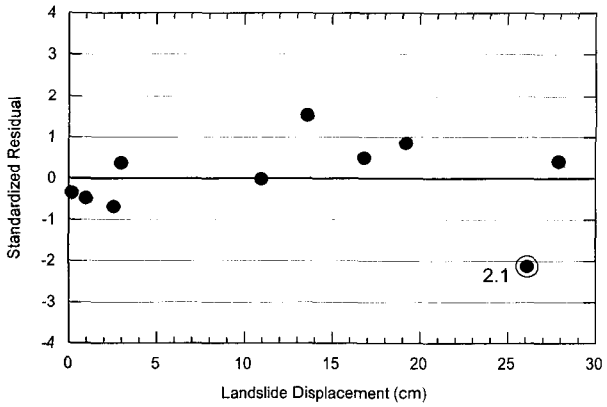

Fig. 8. Standardized residual vs. landslide displacement

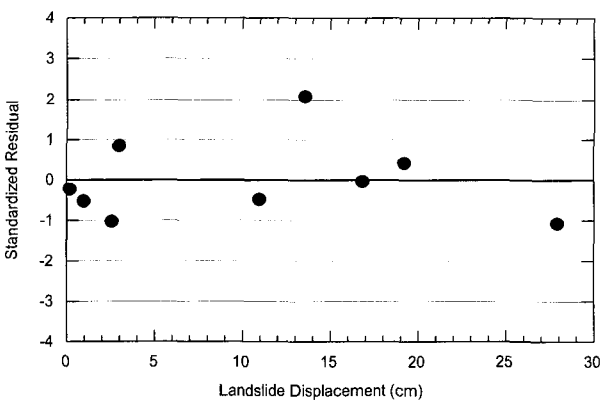

Fig. 10. Standardized residual vs. landslide displacement without bias

useful.

Fig. 7 shows the linear regression of RR versus landslide displacement for maximum adjacent slopes greater than 18° for ϕ' = 30°. It should be noted that the regression line is strongly influenced by one data point, which is marked with a surrounding open circle. Fig. 8 shows from the plot of standard residuals that the data point emphasized in Fig. 7 is a statistical outlier that is 2.1 times the standard deviation from the predicted regression value.

In Fig. 9, the linear regression for ϕ' = 30° is plotted with the statistical outlier removed. The coefficient of determination, r^2, improves markedly. In Fig. 10, the standard residuals for the new regression are shown to be distinguished without obvious bias within very low fraction of the standard deviation from the linear trend line.

Fig. 11 shows the linear regressions of RR versus landslide displacement for various assumed ϕ', ranging from 30° to 40°. Two characteristics of the regressions are apparent. First, the r^2 is not sensitive to the ϕ' assumed. This follows from the fact that changing ϕ' does not significantly affect the statistical variability since all critical acceleration, a_c, for a given ϕ' are affected by the same assumed strength parameter. The second observation is that the slope of the linear reg-

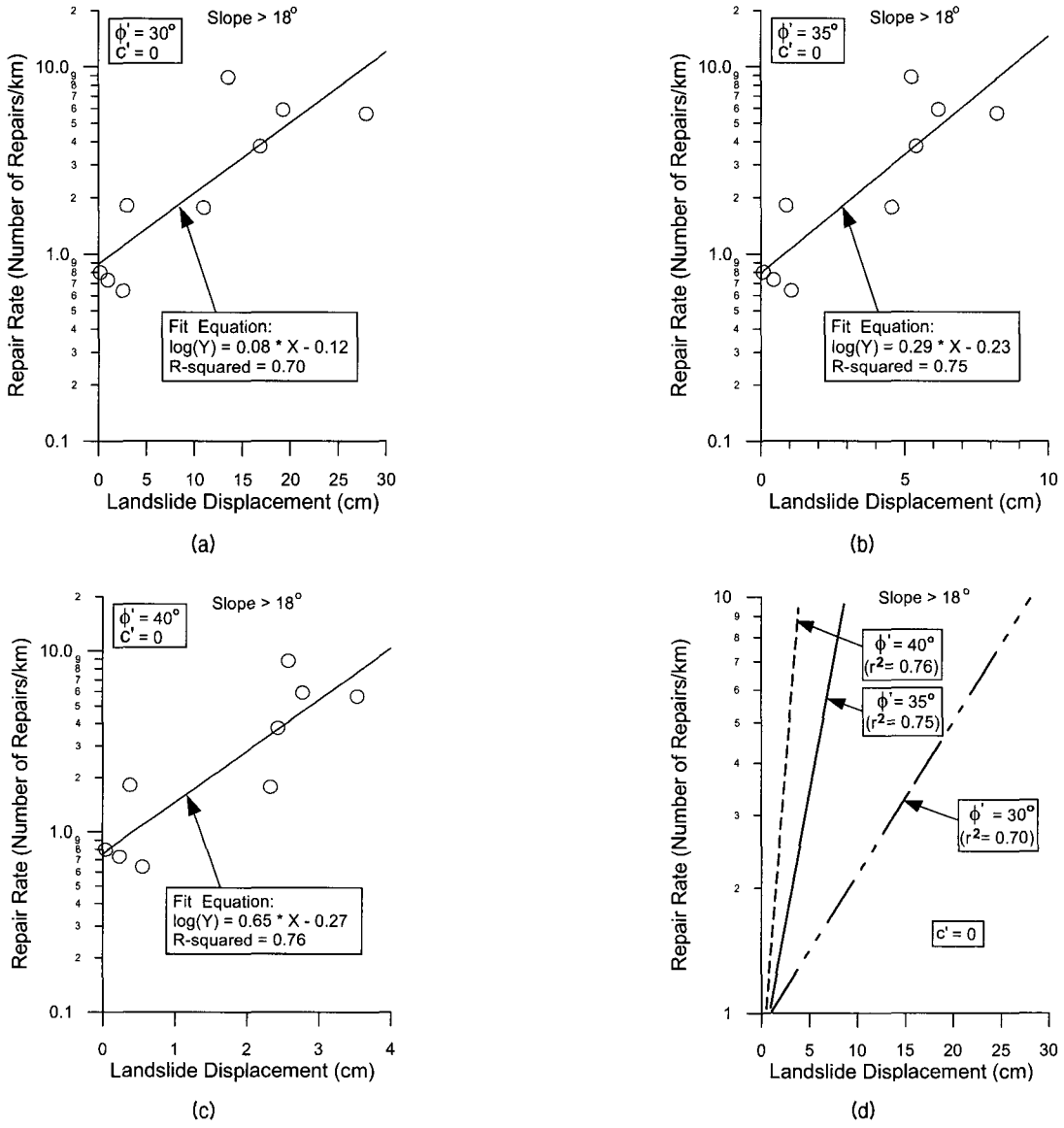

Fig. 11. WSJ steel pipeline repair rate correlation with landslide displacement for various ϕ'

ression increases in direct proportion to ϕ'. This follows because a_c increases as ϕ' increases, and landslide displacement is inversely proportional to a_c. Accordingly, increased ϕ' results in a low estimate of landslide displacement for a given RR, thereby increasing the slope of the linear regression.

In general there is a relatively very good correlation between RR and landslide displacement, with approximately 70% of the variability in the data being explained by the regressions. This characteristic encourages additional work in determining the appropriate c' and ϕ' values associated with the rock formation and soil deposits where the various slopes are located. Although this type of investigation is beyond the scope of this work, strength data related to various soil and rock conditions in the hillsides surrounding the San Fernando have been summarized by Jibson, et al. (1998). These data can be used in conjunction with surficial geology maps to estimate a_c values that are sensitive to local variations in the geology. The refined a_c value can then be used to improve the regressions between repair rate and landslide displacement.

7. Conclusions

The work developed in this study is summarized as follows,

(1) Steel pipelines for water distribution in Los Angeles are concentrated in hillside developments to provide additional resistance against ground deformation triggered by landslide activity. The relationship between the Northridge earthquake steel pipeline repair rates and landslide activity was investigated by regressing repair rate vs. slope angle.

(2) Slope angle was calculated from GIS-based data with digital elevation models (DEMs), which are digital files of cartographic information. Such files were accessed through USGS in 7.5- by 7.5-minute blocks. Elevations data are available in these files on 30-m spacings, from which the slope angle for a 30-m by 30-m area can be calculated. The linear regression between RR and slope was developed. There was no statistically significant relationship between RR and slope for the data set. The regression analysis resulted in a virtual zero slope.

(3) To compensate in part for errors in the locations of the DEMs, pipeline repairs, and pipeline locations, an alternative procedure was developed. Consider the DEM grid. The RR in a particular cell may be affected by the slope in this cell. It may also be affected by the slopes in neighboring cells. In fact, a steep slope in a neighboring cell may be a better measure of the slope geometry driving pipeline repair than the center cell slope. To reflect the influence of slopes in neighboring cells, RRs were correlated with the maximum slope in all cells coincident with or immediately adjacent to the cell for which each RR was calculated. The slope of the linear regression between RR and a maximum slope (α) equal to or less than 18° was essentially zero. Standard statistical tests showed that there is no significant trend for low. In contrast, linear regression for $\alpha > 18^\circ$ shows a very high value of r^2.

(4) The landslide displacement relationship of Jibson, et al. (1998) was used as an index for the combined effects of the angle of slope and AI. Using GIS, the angle of slope at various locations can be determined from DEM files using the estimation model of slope. The AI at various locations in the LA region were estimated by O'Rourke, et al. (1998) and Toprak (1998), and the GIS files of AI developed by them were used. Linear regression of RR and landslide displacement was developed. There is a very good correlation between RR and landslide displacement for maximum adjacent slopes greater than 18°, which accounts for approximately 70% of the variability in the data.

(5) The increased rate of pipeline damage may be related to corrosion effects, which are often most severe for steel pipelines. In addition, steel pipelines are operated by LADWP at significantly higher internal pressures than other types of pipelines.

It should also be noted that significant pipeline damage was observed in cut-and-fill areas (Stewart, et al., 1998). The process of cutting and filling tends to level the ground at a particular location thereby covering the underlying topography with fill that may have a relatively small slope in the location of pipeline damage. Even the procedure adopted in this work for correlating RR with maximum adjacent slope will not identify the appropriate slope that affects damage in a cut-and-fill area.

In the future, it may be advantageous to develop empirical loss estimation models for pipeline damage that correlate repair rate with mapped locations of cut and fill. Improved fill mapping and good construction record keeping will be necessary to develop these types of geospatial databases.

Acknowledgements

This research was supported by the Multidisciplinary Center for Earthquake Engineering Research, Institute of Civil Infrastructure System, and the National Science Foundation in the U.S.A. The author would like to express his sincere gratitude to Professor Thomas D. O'Rourke at Cornell University for frequent and helpful comments on this work.

References

1. American Water Works Association (AWWA) (1964), *Steel Pipe Design and Installation*, AWWA Manual M11, American Water Works Association Inc., New York, NY.
2. Arias, A (1970), *A Measure of Earthquake Intensity*, Seismic Design for Nuclear Power Plants, Ed. R. J. Hansen, The M.I.T. Press, Cambridge, MA, pp.438-483.
3. Barrows, A. G., Irvine P. J., and Tan, S. S. (1995), *Geologic Surface Effects Triggered by the Northridge Earthquake*, Woods, M. C. and W. R. Seiple Eds., California Dept. of Conservation, Division of Mines and Geology Special Publication 116, Sacramento, CA, pp.65-88.
4. Dekermenjian, H. (2000), Personal Communications, LADWP, LA, CA.
5. Eguchi, R. T. (1982), *Earthquake Performance of Water Supply Components During the 1971 San Fernando Earthquake*, Technical Report No.82-1396-2a, J. H. Wiggins Company, Redondo Beach, CA, Mar.
6. Harp, E. L. and Jibson, R. W. (1995), *Inventory of Landslides Triggered by the 1994 Northridge, California Earthquake*, Open-File Report 95-213, U.S. Geological Survey, 17p., 2 plates.
7. Harp, E. L. and Jibson, R. W. (1996), "Landslides Triggered by the 1994 Northridge, California earthquake", *BSSA*, Vol.86, No.1B, pp.s319-s332.
8. Jeon, S.-S. (2002), "Earthquake Performance of Pipelines and Residential Buildings and Rehabilitation with Cast-In-Place Pipe Lining Systems", Ph.D. Dissertation, School of Civil and Env. Engrg, Cornell Univ.
9. Jibson, R. W., Harp, E. L., and Michael, J. A. (1998), *A Method for Producing Digital Probabilistic Seismic Landslide Hazard Maps: An Example from the Los Angeles,California Area*, Open-File Report 98-113, U.S. Geological Survey.
10. Katayama, T. and Isoyama, R. (1980), "Damage to Buried Distribution Pipelines During the Miyagi-kenoki Earthquake", *PVP-43*, ASME, New York, NY, pp.97-104.
11. Kayen, R. E., Mitchell, J. K., and Holzer, T. L. (1994), *Ground Motion Characteristics and Their Relation to Soil Liquefaction at the Wildlife Liquefaction Array, Imperial Valley, California*, Technical Report NCEER-94-0026, T.D. O'Rourke and M. Hamada, Eds., NCEER, Buffalo, NY, Nov., pp. 267-283.
12. Kayen, R. E., Mitchell, J. K., and Holzer, T. L. (1997), "Assessment of Liquefaction Potential During Earthquakes by Arias Intensity", *J. of Geotech. and Geoenvironmental Engrg.* Vol.123, No.12, pp.1162-1174.
13. Newmark, N. M. (1965), "Effects of Earthquakes: Geological Society of America Bulletin", *Geotechnique*, Vol.15, No.2, pp.139-160.
14. O'Rourke, T. D., Grubb, D. T., Netravali, A. N., and Trautmann, C. H. (1985), *Evaluating Service Life of Cast Iron Joint Sealing Products and Techniques*, Geotechnical Engineering Report No.85-3, School of Civil and Env. Engrg., Cornell University, Ithaca, NY, May.
15. O'Rourke, T. D. and Jeon, S.-S. (1999), "Factors Affecting the Earthquake Damage of Water Distribution Systems", *Proc. of 5th US Conference on Lifeline Earthquake Engrg.*, Seattle, WA, ASCE, Reston, VA, Aug., pp.379-388.
16. O'Rourke, T. D. and Toprak, S. (1997), "GIS Assessment of Water Supply Damage from the Northridge Earthquake", *Geotechnical Special Publication No.67*, J. D. Frost, Ed., ASCE, New York, NY, pp.117-131.
17. O'Rourke, T. D., Toprak, S., and Sano, Y. (1998), "Factors Affecting Water Supply Damage Caused by the Northridge Earthquake", *Proc. of 6th US National Conference on Earthquake Engineering*, Seattle, WA, Jun., pp.1-12.
18. Stewart, J. P., Seed, R. B., and Bray, J. D. (1996), "Incidents of Ground Failure from the 1994 Northridge Earthquake", *BSSA*, Vol.86, No.1B, Feb., pp.S300-S318.
19. Stewart, J. P., Bray, J. D., Mcmahon, D. J., and Kropp, A. L. (1998), "Structural Fill Performance During the 1994 Northridge Earthquake", *Proc. of NEHRP Conference and Workshop on Research on the Northridge, California Earthquake of January 17*, Los Angeles, CA, 1997, California Universities for Research in Earthquake Engineering, Richmond, CA, Vol.2, pp.173-180.
20. Tan, S. S. (1995), *Landslide Hazards and Effects of the Northridge Earthquake of January 17, 1994 in the Southern Part of the Van Nuys Quadrangle, Los Angeles County, California*, Open-File Report 95-02, Division of Mines and Geology.
21. Toprak, S. (1998), *Earthquake Effects on Buried Lifeline System*,

Ph.D. Dissertation, School of Civil and Env. Engrg., Cornell Univ., Ithaca, NY.

22. Wieczorek, G. F., Wilson, R. C., and Harp, E. L. (1985), *Map Showing Slope Stability During Earthquakes in San Mateo County California*, U.S. Geological Survey.
23. Wilson, R. C. and Keefer, D. K. (1983), "Dynamic Analysis of a Slope Failure from the 6 August 1979 Coyote Lake", CA, Earthquake, BSSA, Vol.73, No.3, pp.863-877.
24. Wilson, R. C. and Keefer, D. K. (1985), *Predicting Areal Limits of Earthquake-Induced Landsliding*, Professional Paper 1360, In Evaluating Earthquake Hazards in the Los Angeles Region An Earth-Science Perspective, U.S. Geological Survey, pp.316-345.

(received on Mar. 2, 2004, accepted on Apr. 3, 2004)